On the noise reduction mechanisms of porous aerofoil leading edges

Paruchuri Chaitanya and Phillip Joseph

Institute of Sound and Vibration Research, University of Southampton, Highfield SO17 1BJ, United Kingdom

Tze Pei Chong

Brunel University, Uxbridge, UB8 3PH, United Kingdom

Matthew Priddin and Lorna Ayton

University of Cambridge, Cambridge, CB2 8PQ, United Kingdom

Abstract

This paper is predominantly an experimental study into the reduction of turbulence - aerofoil interaction noise by the introduction of aerofoil porosity. In this paper we study three scenarios applied to flat plates: (a) when the flat plate is fully porous, (b) when the flat plate is partially porous from the leading edge and (c) when porosity is introduced downstream of the leading edge. This paper shows that the noise reduction spectra collapse when plotted against non-dimensional frequency fl/U, where l is the length of porous section and U is the flow velocity. Narrow band measurements on a partially porous aerofoil have shown that its noise reduction spectra is characterised by a number of narrow peaks. This paper proposes two main mechanisms for explaining this behaviour. The noise reduction mechanisms are validated against noise reductions measured on a realistic aerofoil at relatively low angles of attack. One of the key findings of this paper is that, by using only a single row of holes downstream of the aerofoil leading edge one can obtain significant levels of noise reduction. This use of downstream porosity is specifically shown to be capable of providing low-frequency noise reductions without increasing the radiated noise at higher frequencies.

Keywords: Turbulence-aerofoil interaction noise, Fan Broadband noise, Porous leading edges, Noise reduction mechanisms.

1. Introduction

The broadband noise produced by the fan wake interacting with the outlet guide vanes (OGV's) is one of the dominant noise sources in a turbofan engine. This form of leading edge interaction noise is also known to be important in wind turbines at low frequencies when the blades interact with large-scale atmospheric turbulence. Serrations (undulations) introduced onto the leading edge have been shown to be a highly effective method for reducing broadband interaction noise [1-7]. Reductions of up to 18dB at some particular frequencies and up to 6dB in overall noise have been reported. However, at chord based Reynolds numbers of $2 \times 10^5 - 6 \times 10^5$ and low angles of attacks (AoA=$0^\circ - 3^\circ$), a clear disadvantage with these leading edge geometries is their negative impact on aerodynamic performance and structural integrity ([6]).

This paper deals with an alternative approach for reducing broadband interaction noise that involves introducing porosity at the leading edge. This control principle has previously been investigated experimentally [3, 8-11] and theoretically [12], where significant reductions in broadband interaction noise of up to 10dB were reported at some frequencies.

The reduction in turbulence interaction noise obtained by using a fully porous SD7003 aerofoil was previously investigated by [8]. Commercially available porous materials such as polyurethane foams, metal foams and felts were used in this study. They showed that open-porous materials with low air flow resistivity (high permeability) lead to greater noise reductions, which are attributed to the suppression of pressure fluctuations at the porous leading edge. The authors also observed at chord based Reynolds numbers of $4 \times 10^5 - 7.8 \times 10^5$ and zero angle of attack, a significant decrease in lift and increase in drag compared to the baseline impermeable aerofoil. One of the main reasons for this poor aerodynamic performance is because the entire aerofoil was made porous.

Roger et al [3] also investigated the use of porosity for reducing interaction noise by filling the shell of a hollow NACA-0012 aerofoil with steel wool. Noise reductions of up to 5 dB were reported, even through there was no attempt at optimising of the material parameters.

Sarradj and Geyer[9] further extended the work of [8] by applying symbolic regression to the noise reduction data to establish models for the noise generation of fully porous aerofoils. They showed that leading edge noise radiation due to porous aerofoils depends on the square of the turbulence intensity and shows a dependency on the fifth to sixth power of the flow velocity. More critically, the spectrum of radiated noise was shown to be highly sensitive to the flow resistivity of the porous material.

More recently, Geyer et al. [11] investigated the noise reductions due to porosity introduced by the use of narrow channels of uniform cross section that were run between the suction and pressure sides of the aerofoil. These channels were only applied to about 5% of leading edge in an attempt to reduce aerodynamic losses. At low geometric angles of attack from $0° - 8°$ and chord based Reynolds numbers of 6.5×10^5, noise reductions of up to 8 dB were reported at some frequencies, while the noise was found to increase by between 4 and 5 dB at high frequencies. Reasons for the reduction of noise are investigated in their paper; they attribute the reduction to a number of mechanisms such as, 1) hydrodynamic absorption in which turbulence kinetic energy is dissipated in the holes, 2) an increase in the effective aerofoil thickness in which the mean flow through the pores increases the boundary layer thickness leading to an effective increase in the aerofoil leading edge, which is well known to reduce interaction noise, 3) displaced turbulence in which the turbulence structures impinging on the aerofoil are displaced away from the surface, leading to a reduction in the pressure fluctuations on the surface, and hence, far-field noise.

Another attempt to explain the noise reduction mechanism was proposed by [10] who evaluated the effectiveness of porous materials on a relatively thick NACA-0024 aerofoil for reducing aerofoil interaction noise. Their experimental results show that the use of porous leading edges leads to a reduction in interaction noise in the low-frequency range and an increase at high-frequencies, mostly due to surface roughness noise. From their hot-wire analysis they also showed that the root-mean-square velocity fluctuations in the close vicinity of the leading edge was reduced due to a weaker flow distortion by the porous leading edge, leading to a reduction in radiated noise.

Priddin *et. al.* [12] have predicted analytically the noise radiation from a flat plate comprising a number of circular holes interacting with a harmonic vortical gust. The Wiener-Hopf method was used to provide the solution and a homogenised impedance-type boundary condition was applied in which the mass flow rate through the holes was related to the jump in velocity potential across the holes via an impedance term related to the Rayleigh conductivity. We note that in this formulation the effects due to viscous dissipation, by vortex shedding for example, are not included and only the real value of the impedance is considered. Predictions were compared against the measured noise reduction spectra from a flat plate comprising of a number of regularly spaced circular holes distributed between the leading edge and some downstream location. In [12] the noise reduction spectra were predicted to peak at the non-dimensional frequencies of fl/U=0.5 and 1.5, where l is the length of the porous section. Narrow band peaks of very similar spectral shape were also observed in the measured data but at the slightly different frequencies of fl/U=0.7 and 1.4. More critically, the predicted frequencies are in the ratio of 1:3, while the peaks in the experimental noise reduction spectra are in the ratio 1:2. The reasons for the existence of these peaks and the difference in the predicted and measured ratios are discussed in this paper, and will be shown to be important in explaining the fundamental noise reduction mechanism.

In this paper we demonstrate that, in addition to the dissipative mechanisms proposed by [10, 11] there are two other potentially more important noise reduction mechanisms. These mechanisms are particularly important for thin aerofoils typical of OGV's, that are non-dissipative but essentially involve interference effects along the chord. In the present paper, the fundamental noise reduction principles are investigated experimentally on a porous flat plate and later extended to a 10% thick aerofoil.

A simple noise reduction model is proposed to explain the basic characteristics of the noise reduction spectra that is entirely consistent with the experimental data. In section 4 of this paper we demonstrate that simply introducing a single row of holes downstream of the leading edge provides similar noise reduction characteristics to that when the aerofoil is fully porous. Naturally, the advantage of this approach is that it requires a much smaller modification to the leading edge and is therefore beneficial for the aerodynamic performance.

2. Noise reduction mechanisms for a fully porous, and partially porous aerofoils

In this section we present a simple and highly idealised model aimed at explaining the dominant noise reduction mechanisms on partially and fully porous aerofoil leading edges. We propose two principal noise reduction mechanisms:

The first mechanism, which is pertinent to fully or partially porous aerofoils, is based on the assumption that by allowing the upper and lower aerofoil surfaces to 'communicate', the unsteady pressure difference Δp across the aerofoil is forced to propagate along the aerofoil chord at the boundary layer convection flow speed U_c. By contrast Δp across a rigid aerofoil propagates at the supersonic speed $a + U_c$, corresponding to the sound speed a in the reference frame moving at U_c in the boundary layer. The important consequence of this phenomenon is that, at subsonic flow speeds $U_c < a$, the surface pressure response by the porous aerofoil radiates with considerably less efficiency compared to the corresponding rigid aerofoil. In this idealised model, zero radiation is predicted when there is an integer number of whole hydrodynamic wavelengths U_c/f across the porous section of length l, i.e., when $fl/U_c = n$, where n is any integer.

The second mechanism is relevant only to partially porous aerofoils in which the noise is reduced through destructive interference between sound generated at the edge discontinuity between the porous section and the downstream rigid

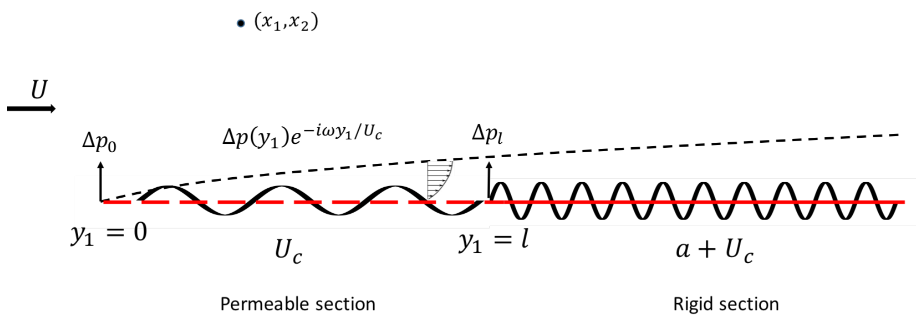

Figure 1: Schematic of the source regions for a partially porous flat plate leading edge.

section, and the sound radiated from the leading edge.

2.1. Simple analytical model

Consider a flat plate aligned along the y_1-direction in the direction of the mean flow with leading edge at y_1=0, as shown in Fig. 1. The flat plate is assumed to be porous over the section $0 \leq y_1 \leq l$, and perfectly rigid for $y_1 \geq l$, assumed to extend to infinitely in the streamwise direction. Turbulent flow impinging on the flat plate leading edge at the flow speed U is assumed to generate three distinct sources. The first occurs when the vortical flow impinges on the leading edge at $y_1 = 0$, which we assume generates a localised compact pressure jump at the leading edge equal to $\Delta p_0 \delta(y_1)$, where δ is the Dirac delta function. The second source is assumed to be of the form of a wave propagating across the porous section $0 < y_1 < l$ at the convection speed U_c. At a single frequency, this source is of the form $\Delta p(y_1)\mathrm{e}^{-\mathrm{i}\omega y_1/U_c}$. Finally, a source is generated at the edge discontinuity $y_1 = l$ between the porous and non-porous (rigid) sections, which, at a single frequency, we represent as a localised compact source of the form, $\Delta p_l \delta(y_1 - l)\mathrm{e}^{-\mathrm{i}\omega l/U}$, whose phase difference compared with the leading edge source at $y_1 = 0$ arises from the time taken l/U for the vortical gust to convect across the porous section of distance l. A schematic of these assumed source distributions is shown in Fig. 1.

Substituting the sum of the two contributions to $\Delta p(y_1)$ discussed above into the chord-wise radiation integral due to Amiet [13] and integrating over the porous section of the aerofoil gives the following expression for the far-field acoustic pressure $p(x_1, x_2, \omega)$,

$$p(x_1, x_2, \omega) \approx \frac{x_2}{4\pi a \sigma^2} \int_0^l \left[\Delta p_0 \delta(y_1) + \Delta p(y_1) \mathrm{e}^{-\mathrm{i}\omega y_1/U_c} + \Delta p_l \delta(y_1 - l) \mathrm{e}^{-\mathrm{i}\omega l/U} \right] \mathrm{e}^{-\mathrm{i}\frac{\omega}{a\beta^2}\left(M - \frac{x_1}{\sigma}\right) y_1} \mathrm{d}y_1 \tag{1}$$

where (x_1, x_2) is the observer position relative to the leading edge with streamwise distance x_1, and transverse distance x_2, $\sigma^2 = x_1^2 + \beta^2 x_2^2$, $\beta^2 = 1 - M^2$ and $M = U/a$.

2.2. Cutoff radiation from porous section

We first consider the radiation from a porous flat plate section of length l, with pressure jump characterised by a wave response convecting with the boundary layer convection speed U_c, $\Delta p(y_1)\mathrm{e}^{-\mathrm{i}\omega y_1/U_c}$. Putting $\Delta p_0 = \Delta p_l = 0$, and for simplicity assuming $\Delta p(y_1) = \Delta p_s$ (i.e., the pressure amplitude of Δp is assumed independent of y_1) in Eq. (1), and after integration, yields

$$p(x_1, x_2, \omega) \approx \frac{x_2 \Delta p_s}{4\pi a \sigma^2} \left[\frac{1 - \mathrm{e}^{-\mathrm{i}\omega l/U_c\left(1 + [M/\beta^2](M - x_1/\sigma)\right)}}{\omega l/U_c \left(1 + [M/\beta^2](M - x_1/\sigma)\right)} \right] \tag{2}$$

The radiated sound power W is related to the mean square far-field pressure integrated over some suitable closed surface:

$$W(\omega) \propto \overline{p^2}(\omega) \propto \mathbf{E}[p^*(\omega) p(\omega)],$$

Comparing this expression to the mean square radiated pressure $\overline{p_{bl}^2}(x_1, x_2)$ in the absence of porous treatment obtained by putting l=0 in Eq. (2), the corresponding reduction in the radiated sound power obtained through cutoff radiation is of the form,

$$\frac{W}{W_{bl}} \propto \frac{\overline{p^2}}{\overline{p_{bl}^2}} = \mathrm{sinc}^2 \left\{ \frac{\omega l}{2U_c} \left[1 + \frac{M}{\beta^2} \left(M - \frac{x_1}{\sigma} \right) \right] \right\} \tag{3}$$

where $\mathrm{sinc}(X) = \sin(X)/X$. We emphasise that Δp_s for the porous and baseline cases will of course differ significantly and Eq. (3) therefore cannot provide a prediction of the absolute noise reduction but is sufficient to predict the main characteristics of the noise reduction spectra.

One of the most significant features of Eq. (3) for the acoustic radiation due to cutoff effects is that the noise reduction spectra are predicted to collapse on fl/U_c and that zero far-field radiation is predicted at frequencies $f_n l/U_c \approx n$ $(n = 1, 2, 3, 4 \ldots)$. Note that the radiated field due to cutoff effects is predicted to oscillate around the general frequency decay $\overline{p^2}(x_1, x_2) \approx (\omega l/U_c)^{-2}$ and therefore the radiation is predicted to tend to zero as frequency increases.

2.3. Edge-to-edge interference

In addition to the cutoff radiation from the porous section, destructive interference will also occur between sound generated at the edge discontinuity between the porous section and the downstream rigid section, and the sound radiated from the leading edge. This is described by the remaining two terms in Eq. (1).

The far-field pressure due to interference from these two sources may be obtained by putting $\Delta p(y_1) = 0$ in Eq. (1) and for simplicity assuming identical edge source strengths $\Delta p_0 = \Delta p_l$. After performing the integration over y_1, the acoustic pressure due to edge-to-edge interference is of the form,

$$p(x_1, x_2, \omega) \approx \frac{x_2 \Delta p_0}{4\pi a \sigma^2} \left(1 + \mathrm{e}^{-\mathrm{i}\omega l/U}\right) \mathrm{e}^{-\mathrm{i}\frac{\omega}{a\beta^2}\left(M - \frac{x_1}{\sigma}\right)l} \tag{4}$$

The two edge sources therefore differ in phase by an amount equal to the time taken l/U for the surface pressure response to travel between the leading edge and the end of the porous section plus the difference in propagation times $l/(a\beta^2)\,(M - x_1/\sigma)$. We note that turbulence is convected between the edges at the free stream velocity U. The corresponding reduction in radiated sound power is therefore given by,

$$\frac{W}{W_{bl}} \propto \frac{\overline{p^2}}{\overline{p^2_{bl}}} = \cos^2\left\{\frac{\omega l}{2U}\left[1 + \frac{M}{\beta^2}\left(M - \frac{x_1}{\sigma}\right)\right]\right\} \tag{5}$$

As in Eq. (5) for the radiation due to cutoff effects the noise radiation due to the edge-to-edge interference is also predicted to collapse on the non-dimensional frequency fl/U, although it is now defined with respect to the free stream velocity U. At sufficiently small values of M, therefore, or when the average pressure is taken over a number of microphones, perfect cancellation of the far-field pressure is predicted at frequencies, $f_n l/U \approx n$-1/2, (n=1, 2, 3, ...). We note that these frequencies differ from those due to source cutoff given by $f_n l/U_c \approx n$, thereby allowing the effects due to the two different mechanisms to be separated.

This assumption of compact sources at the two edge discontinuities cannot be justified from the classical rigid flat plate theory. The edge-to-edge interference condition of Eq. (5) when expressed in terms of non-dimensional acoustic frequency is given by $f_n l/a = (n - 1/2)M$ so that the first interference peak in the noise reduction spectra is $f_1 l/a = M/2$, which at the Mach number $M = U/a$ of the experimental data presented below is $f_1 l/a = 0.075$. The source distribution $\Delta p(y_1)$ for a rigid flat plate is therefore predicted to be uniformly distributed across the porous flat plate and not concentrated at the edges as assumed in the simple model. However, from the measured noise reduction spectra we must assume that the source distribution across the porous section is significantly different compared to a rigid plate. This difference may be explained by a reduction in $\Delta p(y_1)$ downstream of the leading edges, when the unsteady pressures on the upper and lower sides are equalised through communication of the upper and lower pressures across holes. As a result the sources are concentrated at the leading edges, as assumed in the simple theoretical model.

We emphasise that in making the assumption of compact source and equal source strength at either ends of the porous section we are concerned with capturing the general behaviour of the noise reduction spectra and not the absolute levels of the noise reduction that would require more detailed information about the source strength distribution over the porous section.

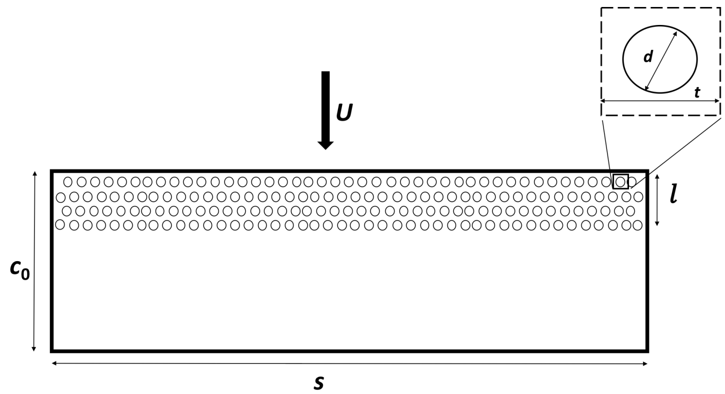

Figure 2: A schematic sketch of porous leading edge profile.

3. Noise reduction mechanism validation

3.1. Porous flat plate and aerofoil configurations

By way of validation of the noise reduction principles outlined above a simple experimental study was undertaken using porous flat plates placed within a turbulent stream. The effect on the radiated noise due to variations in porous leading edge length l and flow velocity U were investigated. A partially porous leading edge on a 3D aerofoil was also investigated to establish whether the same noise reduction principles can be extended to relatively thick aerofoils.

A schematic of the porous flat plate is shown in Fig. 2. Here, a regular pattern of circular holes of diameter d, separated by a distance t are introduced onto a flat plate of 2 mm thickness, span 450 mm and chord c_0, which is varied in the experiment. The length of the porous section from the leading edge is l. In this preliminary study two different configurations were investigated. The first was a fully porous flat plate (i.e., $l = c_0$) with d =3 mm, t = 5 mm (representing a 32% porosity) with c_0 =100 mm and 150 mm. The second was a partially porous flat plates comprising of varying porous length sections, in the range $l/c_0 = 0.2$ to 1, as shown in Fig. 3a.

To verify the same basic noise reduction principles observed in the simple flat plate experiment, porous treatments were also applied to the leading edge of

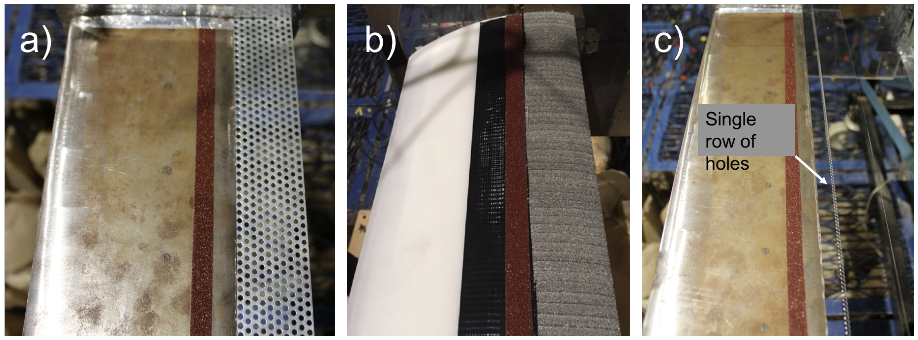

Figure 3: A photograph of the porous LE aerofoil in anechoic wind tunnel a) Partially porous flat plate b) 3D porous leading edge c) Single-row of holes on leading edge (discussed in section 4).

a realistic aerofoil of 10% thickness. Here, the first 50 mm of a NACA 65(12)-10 aerofoil of 150 mm total chord and was replaced by a porous section of identical geometry cut from a metal foam with 90% porosity, as shown in Fig. 3b. The pore diameter of the porous section was in the range of 0.2 to 0.4 mm. The main body was fabricated using a 3-D printer from the durable acrylonitrile butadiene styrene (ABS) photo polymer that has a high-quality surface finish.

3.2. Experimental procedure and instrumentation

Far-field noise measurements were carried out at the Institute of Sound and Vibration Research's open-jet wind tunnel facility. The wind tunnel is located within the anechoic chamber, of dimension 8 m x 8 m x 8 m. The nozzle has dimensions of 150 mm and 450 mm and provides a maximum flow speed of 100 ms^{-1}. A detailed description of the wind tunnel, including its characteristics, is presented by [14].

Far-field noise measurements were made using 16, half-inch condenser microphones (B&K type 4189) located at a constant radial distance of 1.2 m from the mid span of the flat plate leading edge. These microphones were placed at emission angles of between 40° and 130° measured relative to the downstream jet axis. Noise reductions are presented in terms of the Sound Power Level spectra PWL(f) calculated by integrating the pressure spectra over the polar array of 16 microphones using the procedure described in [15]. Measurements were carried for 20 s duration at a sampling frequency of 40 kHz, and the noise spectra were calculated with a window size of 1024 data points corresponding to a frequency resolution of 19.5312 Hz and a bandwidth–time (BT) product of approximately 400, which is sufficient to ensure negligible variance in the spectra estimated at this frequency resolution.

In an attempt to produce turbulence that is approximately homogeneous and isotropic at the aerofoil leading edge, a bi-planar rectangular grid ([16]) of wooden bars of 12 mm width separated by 34 mm was used to generate turbulent inflow. A comparison of the streamwise velocity spectra measured at 145 mm from the nozzle exit plotted against f/U is compared in Fig. 3 of [6] to the theoretical Liepmann velocity spectrum, where the mean square velocity and integral length scale are chosen to give the best fit to the measured data. Close agreement is observed at an inflow condition of 2.5% turbulence intensity and a 7.5 mm streamwise integral length-scale.

3.3. Fully porous flat plates

The validity of the "source cutoff" hypothesis proposed in Section 2.2 and the derivation of Eq. (3) to predict the noise reduction spectra by a fully porous flat plate was investigated by introducing porosity over the entire flat plate. Edge-to-edge interference effects proposed in Section 2.3 were therefore absent in this experiment. The noise reduction spectra were measured by comparing the measured radiation spectra with that obtained from a non-porous flat plate of the same dimensions. Two fully porous flat plates of chord lengths c_0 =100 and 150 mm were investigated at the two different flow velocities of 40 and 60 ms^{-1}. The sound power level reduction spectra for the three cases of (c_0, U)=(100 mm,40 ms^{-1}), (150 mm,40 ms^{-1}) and (150 mm,60 ms^{-1}) are plotted against the non-dimensional frequency fl/U_c, where $l = c_0$ in this case. Also shown in Fig. 4 is the theoretical curve of Eq. (3) for the noise reduction spectra due to cutoff effects, where we have assumed $U_c = 0.7U$ ([17]).

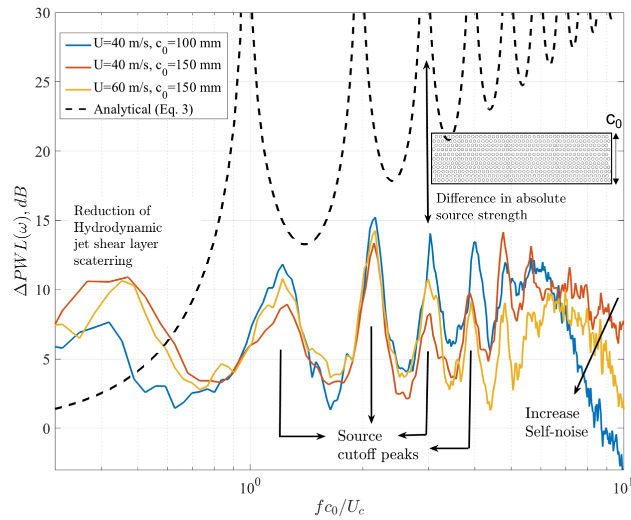

Figure 4: Sound pressure level reduction spectra versus non-dimensional frequency fc_0/U_c measured flow speeds of 40 and 60 ms^{-1} for a fully porous leading edge of length 100 mm and 150 mm. Also shown is the theoretical curves for the source cutoff noise reduction mechanism.

Excellent collapse of the three measured spectra are observed with each spectra clearly showing evidence of multiple peaks of maximum noise reduction of up to 15dB at $fl/U_c = 1.2, 2.1, 3.0, 3.9, 4.8, \ldots$. These peak frequencies are entirely consistent with the hypothesis of source cutoff proposed in Eq. (3) where peak noise reductions corresponding to $fl/U_c \approx n$ are predicted. The small difference between the measured and predicted frequencies can be attributed to variations in convection velocity and its frequency dependence where variations of up to 20% can be observed on aerofoil geometry. [18]. Naturally, the simple theory considerably over-estimates the measured noise reductions owing to the idealised assumptions made regarding their relative source strengths. Moreover, the predictions do not include the effects of additional noise sources generated by the porous plate, such as roughness noise and the noise due to the cross-flow effects. Nevertheless, the agreement is sufficiently close to provide confidence in the proposed noise reduction mechanism. Note that the levels of noise reductions appear to diminish as the chord length c_0 is increased. This may be due to reduction in the coherence of Δp along the chord with the increase of chord length.

3.4. Partially porous leading edges

We now investigate experimentally the noise reduction spectra due to partially porous flat plates in which, according to our hypotheses in Section 2, two distinct noise reduction mechanisms are involved. In Section 2.3 we argue that edge-to-edge interference is also present when the aerofoil is only partially porous. To validate this hypothesis the noise reduction spectra were measured for a range of different porous section lengths l/c_0=0.2, 0.32, 0.49 on a flat plate at $U = 60$ ms^{-1}. Sound power level reduction spectra are plotted in Fig. 5 versus fl/U for a fixed chord length of 150 mm. It is clear from this figure that introducing porosity on only the leading edge section of the aerofoil introduces additional peaks compared to that when it is fully porous. Now present in figure are the peaks fl/U=0.5 and 1.5 in addition to the source cutoff peaks of fl/U_c=1.2, 2.1 (equivalent to fl/U=0.85, 1.4 based on the assumption of $U_c = 0.7U$). These additional peak frequencies are in excellent agreement with the predicted peaks from Eq. (5) based on the assumption of destructive interference between the two edge discontinuities at $y_1 = 0$ and l. Moreover, a good collapse is observed when the measured noise reduction peaks are plotted against fl/U. Considerably better agreement with the measured noise spectra may be obtained by allowing the source strengths at the ends of the porous section to vary by a non-dimensional frequency-dependent complex factor η whose phase will cause a shift in the peak frequencies and whose magnitude will affect the noise reduction peaks, i.e., $\Delta p_0 = \eta \Delta p_l$. Infinitely large noise reductions are predicted for η=1 which then reduces as η deviates from 1. This ability to shift noise reduction peaks is also possible in the more complicated Wiener-Hopf model of Priddin *et. al.* [12], whereby a complex impedance parameter would result in an additional phase term which would also allow for a shift in peak frequencies. However, this effect is a comparatively minor effect and for simplicity we consider η=1.

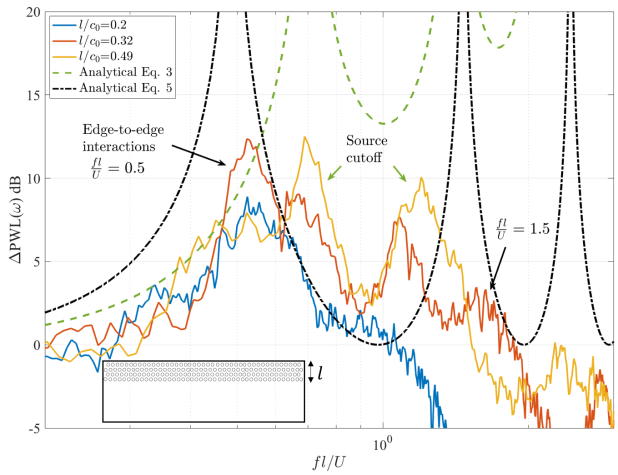

Figure 5: Sound pressure level noise reductions versus non-dimensional frequency fl/U for partially porous flat plates of varying porous length of l/c_0=0.2, 0.32 and 0.49 at the flow velocity of 60 ms^{-1}. Also shown are the theoretical curves for the two noise reduction mechanisms.

Figures 4 and 5 showing the noise reduction spectra for both fully and partially porous flat plates, and their collapse on fl/U, have provided strong validation of the two noise reduction mechanisms proposed above. The level of noise reductions appear to improve as l is increased which may be related to the sources being more localised at the edges $y_1 = 0$ and $y_1 = l$.

We conclude this section by demonstrating that the same fundamental noise reduction principles observed in the simple flat plate measurements are also present in a realistic and relatively thick, aerofoil with porous leading edges. Porosity was introduced into the first 5 cm of a NACA65 aerofoil of 150 mm total chord and 10% thickness (see Fig. 3b). The variation in noise reductions due to changes in the porous section length l was investigated by the use of thin metal tape to cover both the upper and lower surfaces of the porous section. Three values of l were investigated corresponding to 10, 20 and 30% of the chord (l= 1.5, 3.0 and 4.5 cm). The sound power level reduction spectra plotted against fl/U at a flow speed of 40 ms^{-1} and AoA=0° for the three section lengths of

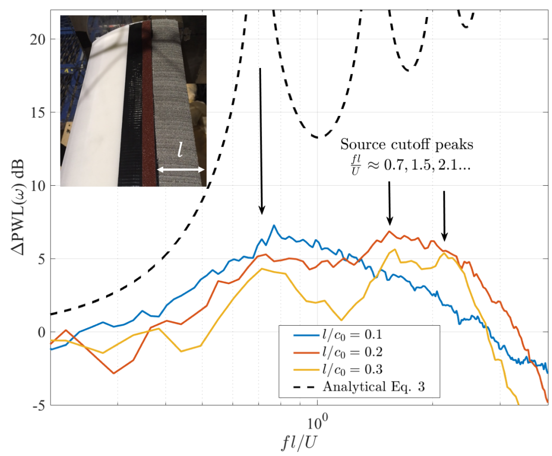

Figure 6: Sound power level reduction spectrum for a NACA65 aerofoil with 5cm, 10cm and 15cm of porous leading edge versus non-dimensional frequency fl/U measured at 40 ms^{-1} and AoA=0°. Also shown is the theoretical curves for the dominant noise reduction mechanism.

l/c_0 of 0.1, 0.2 and 0.3 are shown in Fig. 6. Also shown in this figure is the theoretical curve of Eq. (3).

The noise reduction spectra are observed to have similar behaviour to the flat plate spectra in Fig. 5 and collapse reasonably well on fl/U. Peaks at fl/U ≈0.7, 1.4 and 2.1 (corresponding to $fl/U_c = 1, 2, 3\ldots$ assuming $U_c = 0.7U$) are also observed in the noise reduction spectra for the two largest porous sections. The second peak in the measured noise reduction spectra is absent for the shortest porous section due to masking by self-noise source at this relatively high (absolute) frequency. For the two largest porous sections, the second peak is marginally greater than the first peak by about 1dB suggesting that the cutoff effect is the dominant noise reduction mechanism for this choice of geometry and porosity.

It is important to note the absence of peaks at $fl/U = n - 1/2$ resulting from the edge-to-edge interaction noise for this 3D aerofoil. We can conclude therefore that the sources at $y_1 = 0$ and $y_1 = l$ are sufficiently different in level, or sufficiently weak, so that their level of destructive interference is negligible.

Edge-to-edge interference is therefore not a dominant noise reduction mechanism for this relatively thick aerofoil and porosity but may be more significant in other configurations. Another possible noise reduction mechanism is the Helmholtz-type resonance created by the mass of tape acting against the stiffness of the air trapped by the tape on both sides of the porous leading edge. However, it is not clear at the present time how this type of resonance can lead to noise reductions and occur at harmonic frequencies.

Finally, we investigate the effect on the noise reductions due to changes in angle of attack of the NACA65 aerofoil. Fig. 6 shows the sound power level reduction spectra plotted against fl/U for a fixed porous length of $l/c_0 = 0.3$ at three different geometric AoA=0°, 5°, 10° and a flow speed of 40 ms^{-1}. The noise reduction spectra are observed to have similar behaviour to the AoA=0° spectra in Fig. 6 and collapse reasonably well on fl/U except at high frequencies $fl/U \geq 1.5$. With the increase of AoA, a significant increase in the radiated noise is observed and may be attributed to the increase in self-noise due to cross-flow through the porous section. This cross-flow effect can be avoided by the introduction of a solid plates passing through mid-camber line as demonstrated by [10]. Note that in this study the effective angles of attack are very small due to jet deflection from the open-jet wind tunnel measurements.

In the next section we propose an alternative porosity distribution for the reduction of broadband leading edge interaction noise. The innovative feature of this porous configuration is that the porous section is located well downstream of the leading edge and is therefore predicted to have much smaller effect on the aerodynamic performance. We now demonstrate that this new porosity configuration is able to reproduce the same cutoff radiation effects demonstrated previously for the partially porous aerofoils.

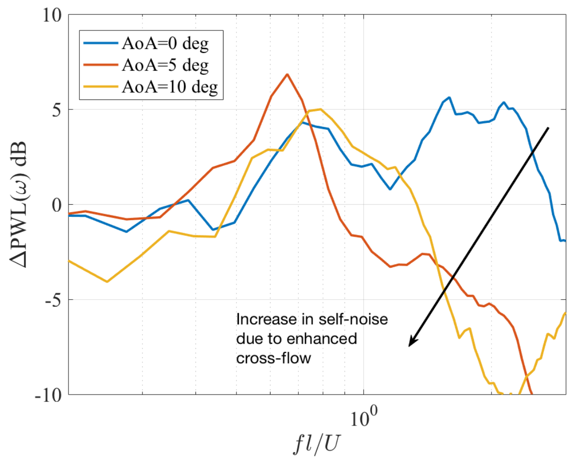

Figure 7: Sound power level reduction spectrum for a NACA65 aerofoil with 15cm of porous leading edge versus non-dimensional frequency fl/U measured at 40 ms^{-1} at AoA=0°, 5°, 10°.

4. Porosity downstream of the leading edge

4.1. Flat plate configurations

In this section we explore the effect on noise reduction performance obtained when holes are introduced downstream of the leading edge of a flat plate. In the general case a porous section of length l is located at a distance of l_0 from the leading edge of the flat plate, as shown in Fig. 2 and Fig. 3c. A total of 40 different porous plates of varying hole diameters d, hole spacing t, number of porous rows, rectangular slot geometry and distance from the leading edge l_0 were tested. Table 1 provides a summary of the flat plate configurations tested in this study.

Configuration	Hole diameter, d (in mm)	Spacing (t/d)	Distances (in mm)
Single row	1, 2, 3 and 4	1.5, 2, 2.5 and 3	l_0=40, 60, $l = d$, c_0=150
2 rows	2	2	l_0=40, 60, $l = 2d + t$, c_0=150
3 rows	2	2	l_0=40, 60, $l = 3d + 2t$, c_0=150

Table 1: A summary of flat plate experiments performed in the current study.

4.2. Noise reduction performance

Figure 8 shows the typical noise reduction spectra plotted against fl_0/U for a single row of holes of d =2 mm and t =4 mm at the four different locations of l_0/c_0=0.13, 0.2 and 0.27 and 0.4 at a fixed velocity of 40 ms^{-1}.

Even though only a single row of holes are introduced well downstream of the leading edge, the noise reduction spectra exhibit similar characteristics, but at a lower level, to that obtained when an entire porous section of length l is introduced. Good collapse of the spectra is obtained when plotting against fl_0/U. Unexpectedly, peak frequencies at fl_0/U ≈0.7, 1.4 and 2.1 are observed which are identical to that obtained for partially porous sections of length l as shown in Fig. 5.

Clearly, therefore, a single row of holes located downstream of the leading edge provides a noise reduction mechanism similar in principle to that when the aerofoil is partially porous. We argue above that this mechanism is mainly due to the unsteady aerofoil response now convecting with the flow speed rather than the sound speed for rigid aerofoils. The reasons for this behaviour is currently unknown but we speculate that introducing downstream porosity creates a local low-pressure boundary condition $\Delta p(l_0) \approx 0$ which has a significant effect on $\Delta p(y_1)$ upstream. It is possible that forcing $\Delta p(y_1)$ to be small at $y_1 = l_0$ forces a slowing of $\Delta p(y_1)$ to that of the flow speed. Clearly, more work is needed to confirm this hypothesis, although at the present time we are unable to provide an alternative explanation behind these peak frequencies. We note that another benefit in relocating the porosity downstream of the leading edge is a reduction in the noise increase at high frequencies. The precise reason for this finding is also not known but may be related to reduced roughness noise or a thinner boundary layer associated with holes introduced further downstream.

The influence of the hole diameter was also investigated where a very small hole of just d =1mm in diameter was found to achieve similar noise reductions to within 1dB at most frequencies and up to 3dB at the peak frequencies. An increase in hole diameter was also found to increase self-noise at high frequencies, which may be related to increased roughness. Varying the hole, spacing and

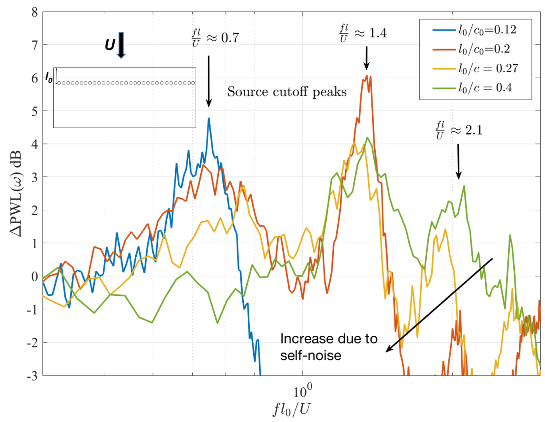

Figure 8: Sound pressure level reduction spectra versus non-dimensional frequency fl_0/U measured at a flow speed of 40 ms^{-1} for a single row of holes located at distances $l_0/c_0 =$ 0.12, 0.2, 0.27 and 0.4 from the leading edge.

replacing the circular holes with rectangular slots was found to have a negligible effect ($\leq$ 1.5dB) on the noise reduction levels.

Finally, we investigate the most general configuration in which a porous section of length l is introduced at a distance of l_0 downstream of the leading edge. Figure 9 shows the comparison of the sound power reduction spectra obtained using 5 rows of holes of d =3 mm and t=5 mm located at $l_0/c_0 = 0$ and l_0/c_0 =0.32 whose length of porous section is l/c_0 =0.32 at a flow velocity of 40 ms^{-1}. The effect of relocating the holes downstream can be seen to provide a significant reduction (of up 5dB) in noise over a same band of frequencies to that obtained when the holes are introduced at the leading edge. These reductions are superior to those in Fig. 4 where only a single row of holes are used. However, the significant difference now is that the two spectral peaks are absent. Clearly, the introduction of an additional edge discontinuity at $y_1 = l + l_0$ has the effect of modifying the source balance and weakening the effects of destructive interference such that strong interference peaks no longer occur. However, the important difference between the two cases is that at the leading edge, where most of the lift is generated, does not require significant modification, which

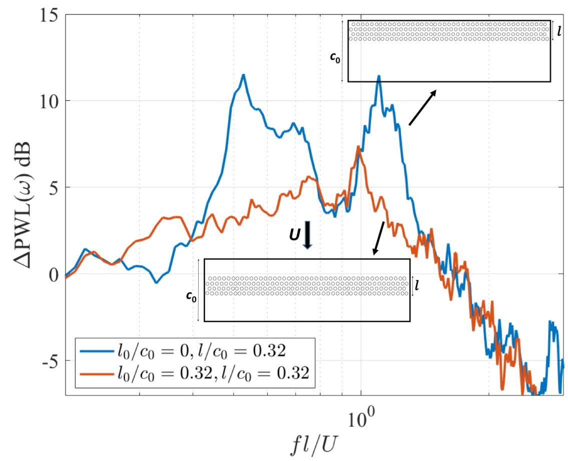

Figure 9: Sound pressure level reduction spectrum versus non-dimensional frequency fl/U measured at a flow speed of 40 ms^{-1} to demonstrate the influence of porous section introduced downstream of the leading edge.

should have significant benefit in terms of aerodynamic performance.

5. Conclusion

This paper has investigated in detail the reductions in the broadband aerofoil interaction noise due to the introduction of porosity over the entire chord, over a short section from the leading edge and a short section located downstream of the leading edge. Consistent with the results from the previous work, porous leading edges have been shown to provide substantial reductions in turbulence-aerofoil interaction noise. This paper has shown experimentally and through a simple analytic model that noise reduction spectra strongly collapse when plotted against non-dimensional frequency fl/U. Narrow band measurements for a partially porous aerofoil have shown that its noise reduction spectrum is characterised by a number of narrow peaks at approximately $fl/U_c \approx n$ and $fl/U \approx n - 1/2$, where n is any integer. This paper has proposed two main mechanisms for explaining this behaviour. The first is a 'Source cutoff' effect in which the unsteady aerofoil response is assumed to convect at the flow convection speed and therefore radiates with much lower efficiency than for a rigid aerofoil whose unsteady response is at supersonic speeds. The second mechanism invoked to explain the observed noise reduction spectrum is related to the 'Edge-to-edge interference' in which compact sources at the edge discontinuities interfere destructively.

An intriguing finding of this paper is that just a row of holes downstream of the aerofoil leading edge can provide a similar effect on the noise radiation spectra as when the aerofoil is made partially porous from the leading edge. The cutoff radiation effects have been proposed to explain this behaviour but more work is needed to establish more definitely the noise reduction mechanism.

Acknowledgments

The first author would like to acknowledge the financial support of the Royal Academy of Engineering (RF/201819/18/194) and Oscar Propulsion, specifically Mr. David Taylor. M.J.P. acknowledges support from EPSRC DTP EP/N509620/1. LJA acknowledges support from EPSRC Early Career Fellowship EP/P015980/1.

References

[1] A. Hersh, P. Soderman, R. Hayden, Investigation of acoustic effets of leading edge serrations on airfoils, J. Aircr. 11(4) (1974) 197–202.

[2] T. Geyer, E. Sarradj, J. Giesler, Application of a beam forming technique to the measurement of airfoil leading edge noise, Adv. Acou. and Vibr. (2012) 1–16.

[3] M. Roger, C. Schram, L. De Santana, Reduction of airfoil turbulence-impingement noise by means of leading-edge serrations and/or porous materials, in: 19th AIAA/CEAS Aeroacoustics Conference, no. AIAA 2013-2108, 2013.

[4] J. Kim, S. Haeri, P. Joseph, On the reduction of aerofoil-turbulence interaction noise associated with wavy leading edges, J. Fluid Mech. 792 (2016) 526–552.

[5] B. Lyu, M. Azarpeyvand, On the noise prediction for serrated leading edges, J. Fluid Mech. 826 (2017) 205–234.

[6] P. Chaitanya, P. Joseph, S. Narayanan, C. Vanderwel, J. Turner, J. W. Kim, B. Ganapathisubramani, Performance and mechanism of sinusoidal leading edge serrations for the reduction of turbulence-aerofoil interaction noise, J. Fluid Mech. 818 (2017) 435–464.
URL doi:10.1017/jfm.2016.95

[7] P. Chaitanya, P. Joseph, L. Ayton, Leading-edge profiles for the reduction of airfoil interaction noise, AIAA J. 57(12) (2019) 1–12.

[8] T. Geyer, E. Sarradjy, J. Giesler, M. Hobrachtz, Experimental assessment of the noise generated at the leading edge of porous airfoils using microphone array techniques, in: 17th AIAA/CEAS Aeroacoustics Conference, no. AIAA-2011-2713, 2011.

[9] E. Sarradj, T. Geyer, Symbolic regression modeling of noise generation at porous airfoils, J. Sound Vib. 333 (2014) 3189–3202.

[10] R. Zamponi, D. Ragni, N. V. de Wyer, C. Schram, Experimental investigation of airfoil turbulence-impingement noise reduction using porous treatment, in: 25th AIAA/CEAS Aeroacoustics Conference, no. AIAA-2019-2649, 2019.

[11] T. F. Geyer, A. Lucius, M. Schrödter, M. Schneider, E. Sarradj, Reduction of turbulence interaction noise through airfoils with perforated leading edges, Acta Acust. United Ac. 105 (2019) 109 – 122.

[12] M. J. Priddin, L. J. Ayton, P. Chaitanya, P. Joseph, A semi-analytic and experimental study of porous leading edges, in: 17th AIAA/CEAS Aeroacoustics Conference, no. AIAA-2019-2552, 2019.

[13] R. Amiet, Acoustic radiation from an airfoil in a turbulent stream, J. Sound Vib. 41 (4) (1975) 407–402.

[14] T. P. Chong, P. Joseph, P. O. A. L. Davies, A parametric study of passive flow control for a short, high area ratio 90^o curved diffuser, J. Fluids Eng. 130 (11) (2008) 111104–12.

[15] S. Narayanan, P. Chaitanya, S. Haeri, P. Joseph, J. W. Kim, C. Polacsek, Airfoil noise reductions through leading edge serrations, Phys. Fluids 27 (025109) (2015).

[16] P. E. Roach, The generation of nearly isotropic turbulence by means of grids, Int. J. Heat Fluid Fl. 8(2) (1987) 82–92.

[17] W. K. Blake, Mechanics of Flow-induced sound and vibration, volume 2: Complex flow structure interactions, Academic Press (Elsevier), Paris, 2017.

[18] M. Gruber, Airfoil noise reduction by edge treatments, Ph.D. thesis, University of Southampton, ISVR (2012).